JMeXFRI

Journal of the Mexican Federation of Radiology and Imaging

Check for updates

FULL RESEARCH ARTICLE

Elastographic patterns of thyroid microcarcinomas: a new proposal

Eduardo R. Cuvertino[1,2], Liliana Gelman[1], Mirta Miras-Miartus[3], Alejandra Geres[4], and Maria L. Cuvertino[2,5]*

[1]Departamento de Diagnostico por Imagen, Hospital Nacional de Clinicas de la Facultad de Ciencias Medicas, Universidad Nacional; [2]Centro de Estudios Ecograficos; [3]Servicio de Endocrinologia, Hospital de Niños de la Santisima Trinidad; [4]Servicio de Endocrinologia, Hospital Nacional de Clinicas de la Facultad de Ciencias Medicas, Universidad Nacional; [5]Servicio de Radiologia y Diagnostico por Imagenes, Hospital de Niños de la Santísima Trinidad. Cordoba, Argentina

ABSTRACT

Introduction: *Ultrasound (US) elastography for thyroid microcarcinomas has variable diagnostic performance. This study aimed to (1) define the elastographic features of thyroid nodules using two-dimensional shear-wave elastography (2D-SWE) and (2) evaluate the utility of combining conventional US, elastography-strain (E-strain), and 2D-SWE for improving diagnostic performance in thyroid micronodules.* **Materials and Methods:** *Patients with thyroid nodules were evaluated in a cross-sectional study with conventional US, E-strain, and 2D-SWE. Nodule stiffness, the presence of a perinodular halo, and the halo/nodule A/B index were evaluated using 2D-SWE. Three elastographic patterns were defined based on conventional US, E-strain, and 2D-SWE features. The pathological diagnosis was made by fine needle aspiration biopsy and confirmed by surgery.* **Results:** *We included 158 patients with 158 thyroid nodules: 64 micronodules ≤10 mm and 94 macronodules > 10 mm. Malignancy was confirmed in 58 (36.7%) of 158 nodules, of which 29 were thyroid microcarcinomas. Stiffness at a cutoff value of 23.5 kPa predicted malignancy. Notably, 21 (72.4%) of 29 microcarcinomas with a perinodular halo had a stiffness value of < 23.5 kPa. All microcarcinomas with a perinodular halo (n = 21, 100%) had an elastographic stiffness A/B index ≥ 1.3. A congruent elastographic pattern was defined as thyroid imaging reporting and data system (TI-RADS) 4 or 5, E-strain pattern 4 or 5, with a stiffness ≥ 23.5 kPa without a perinodular halo, and an A/B index < 1.3 by 2D-SWE. An incongruent elastographic pattern was defined as TI-RADS 4 or 5, E-strain pattern 4 or 5, and discordant findings on 2D-SWE with intrinsic thyroid nodule laxity (< 23.5 kPa), a rigid perinodular halo, and an A/B index ≥ 1.3. An atypical congruent elastographic pattern was defined as TI-RADS 4 or 5 with atypical findings on E-strain (pattern 1, 2, or 3), and 2D-SWE with intrinsic thyroid nodule laxity (< 23.5 kPa), a rigid perinodular halo, and an A/B index ≥ 1.3.* **Conclusion:** *Three elastographic patterns of thyroid microcarcinomas are proposed based on 2D-SWE features such as nodule stiffness, a perinodular halo, and an A/B index in combination with conventional US and E-strain. These elastographic patterns have not been described in the literature.*

Keywords: *Thyroid. Elastography. Thyroid microcarcinoma. Thyroid nodule. Ultrasound. TI-RADS.*

Corresponding author:
Eduardo R. Cuvertino
E-mail: ercuvertino@gmail.com

Received for publication: 01-10-2023
Accepted for publication: 12-01-2024
DOI: 10.24875/JMEXFRI.M24000072

Available online: 10-07-2024
J Mex Fed Radiol Imaging. 2024;3(2):82-92
www.JMeXFRI.com

INTRODUCTION

Ultrasound (US) elastography is an additional tool of conventional US examination and fine needle aspiration biopsy (FNAB) that differentiates benign and malignant thyroid nodules, especially the Bethesda III or IV category cytology cases (malignancy risk rates of 5% and 30%, respectively)[1-4]. Two main thyroid elastography methods are used in clinical practice: real-time elastography strain (E-strain), a qualitative technique of manual compression to assess tissue deformity, and shear wave elastography (SWE), a quantitative estimate of tissue stiffness in kilopascals (kPa) or meters/second that shows a color matrix related to tissue stiffness presented as a two-dimensional SWE (2D-SWE)[1,2].

Morphological findings of benign and malignant thyroid nodules are related to the pathological type of the tumor and the size of the lesion[1]. Many malignant thyroid micronodules (≤10 mm) have no obvious morphological changes, which is a problem when conventional ultrasound is used for diagnosis. On the other hand, 2D-SWE has improved the characterization of thyroid nodules with high specificity of tissue stiffness, which positively correlates with nodule malignancy. A malignant thyroid nodule is stiffer than a benign nodule[5]. However, US elastography has variable diagnostic performance in thyroid microcarcinomas.

A few reports have evaluated the diagnostic value of 2D-SWE in thyroid microcarcinomas. Their intrinsic structure may affect stiffness, as measured by elastography, and there is evidence that tissue stiffness is lower in micronodules than in large nodules[5,6]. It has been suggested that elastographic assessment of perinodular tissue can contribute to the differential diagnosis[6]. Therefore, this study aimed to (1) define the elastographic features of thyroid nodules using 2D-SWE and (2) evaluate the utility of combining the findings of conventional US, E-strain, and 2D-SWE for improving diagnostic performance in thyroid micronodules.

MATERIALS AND METHODS

This retrospective cross-sectional study was conducted from May to November 2021 at the Diagnostic Imaging Department of the National Hospital of Clinics, Faculty of Medical Sciences of the National University and Center of Ultrasound Studies, in Córdoba, Argentina. Patients of both sexes with thyroid nodules detected by conventional US were included. The study was approved by the institutional research committee, and written informed consent was obtained from all patients.

Development and study variables

Patients with thyroid nodules were evaluated by grayscale US, color Doppler US, E-strain, and 2D-SWE. The variables were age, sex, Thyroid Imaging Reporting and Data System (TI-RADS) category, and thyroid nodule volume.

Definitions

Micronodule: ≤ 10 mm in diameter on US grayscale.

Macronodule: > 10 mm in diameter on US grayscale.

E-strain pattern: Rago score[8] was used: 1 point indicates the elasticity of the entire examined area of the thyroid nodule; 2 points, the elasticity of a large portion; 3 points, the elasticity only in the periphery; 4 points, the lack of elasticity of the nodule; and 5 points, the lack of elasticity of the nodule and the perinodular area. The green color of the map indicates low stiffness, while the red color indicates non-deformable hard tissue.

Tissue stiffness (kPa): This is the unit of measure of pixel density obtained by 2D-SWE that quantifies stiffness. Stiffness is expressed in a color matrix from blue (soft) to red (hard).

Halo/nodule stiffness index (A/B index): a quantitative measure proposed by the authors (EC and MC) which evaluates the 2D-SWE color matrix. (A) corresponds to the stiffness of an extended region of interest (ROI) that includes the thyroid nodule + a perinodular halo (up to 2 mm outside the nodule boundary). (B) corresponds to the stiffness of the nodule ROI.

Image acquisition and analysis protocol

Thyroid nodule examinations were performed with a Resona 7 ultrasound (Mindray Medical International, Shenzhen, China) and an L14-5 linear transducer with the recent real-time SWE version. This system has a single-layer analysis function that measures stiffness and the margin surrounding the lesion with 0.5 mm increments.

After conventional US examination, elastographic images were acquired in the same section for approximately 4–6 s. The nodule and adjacent thyroid tissue were examined, and thyroid nodules were aspirated. Elastographic acquisitions were performed with E-strain and 2D-SWE five-sequence images. The ROIs (extranodular, intranodular, and perinodular) were selected,

Table 1. Thyroid micronodule and macronodule characteristics by TI-RADS, E-strain, and Bethesda System

Description	Total (n = 158)	Thyroid micronodules[a] (n = 64)	Thyroid macronodules[b] (n = 94)
Women, n (%)	131 (82.9)	54 (84.4)	77 (81.9)
Men, n (%)	27 (17.1)	10 (15.6)	17 (18.1)
TI-RADS, n (%)			
2	19 (12.0)	2 (3.1)	17 (18.0)
3	50 (31.6)	15 (23.4)	35 (37.2)
4	63 (39.9)	35 (54.7)	28 (29.8)
5	26 (16.5)	12 (18.8)	14 (15.0)
E-strain pattern, n (%)			
2	52 (32.9)	16 (25.0)	36 (38.4)
3	34 (21.5)	8 (12.5)	26 (27.6)
4	60 (38.0)	34 (53.1)	26 (27.6)
5	12 (7.6)	6 (9.4)	6 (6.4)
Bethesda System, n (%)			
II	92 (58.2)	28 (43.8)	64 (68.1)
III	12 (7.6)	11 (17.2)	1 (1.0)
IV	7 (4.4)	2 (3.1)	5 (5.3)
V	44 (27.9)	21 (32.8)	23 (24.5)
VI	3 (1.9)	2 (3.1)	1 (1.1)
Pathological diagnosis[c]			
Benign thyroid nodule, n (%)	100 (63.3)	35 (54.7)	65 (69.1)
Malignant thyroid nodule, n (%)	58 (36.7)	29 (45.3)	29 (30.9)

[a]Thyroid micronodule volume on ultrasound was ≤ 10 mm.
[b]Thyroid macronodule volume on ultrasound was > 10 mm.
[c]Confirmed by surgical specimens.
E-strain: elastography strain; TI-RADS: Thyroid Imaging Reporting and Data System.

Table 2. Association between 2D-SWE thyroid nodule stiffness and the cytopathological Bethesda category

Nodule stiffness	Bethesda category				
	II	III	IV	V	VI
n = 158	92	12	7	44	3
kPa, median	18.0	21.5	24.0	27.5	33.0
kPa, mean	18.9	27.5	28.1	29.6	28.00
kPa, SD	6.3	20.4	14.4	11.5	10.4
kPa, minimum	7.0	9.0	14.0	5.0	16.0
kPa, maximum	35.0	80.0	59.0	64.0	35.0
kPa, IQ range	9.0	19.2	8.0	12.7	-

2D-SWE: two-dimensional shear wave elastography; kPa: kilopascals.

Table 3. 2D-SWE nodule stiffness of thyroid microcarcinomas with and without perinodular halo

Nodule stiffness	Nodule stiffness with a perinodular halo (n = 21)	Nodule stiffness without a perinodular halo (n = 8)
kPa, median	21.0	24.5
kPa, mean	21.3	23.8
kPa, minimum	16.0	22.0
kPa, maximum	30.0	25.0
kPa, lower limit 95% CI	17.4	19.8
kPa, upper limit 95% CI	25.3	27.8

2D-SWE: two-dimensional shear wave elastography; kPa: kilopascals; CI: confidence interval.

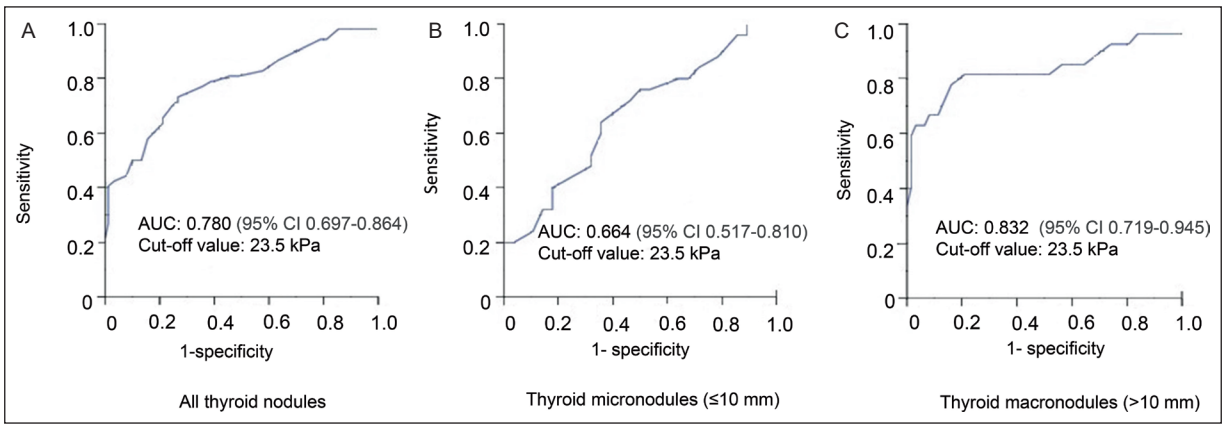

Figure 1. Diagnostic performance of the nodule stiffness cutoff values with 2D-SWE. ROC analyses show a comparison of the 23.5 kPa cutoff value in three groups. **A:** all thyroid nodules. **B:** thyroid micronodules (≤ 10 mm). **C**: thyroid macronodules (> 10 mm). The best performance of the nodule stiffness cutoff value (≥ 23.5 kPa) for predicting malignancy was found in thyroid macronodules (AUC: 0.832). In contrast, the 23.5 kPa cutoff value for thyroid micronodules had an AUC of 0.664.

AUC: area under the curve; CI: confidence interval; kPa: kilopascals; mm: millimeters; 2D-SWE: two-dimensional shear wave elastography; ROC: receiving operating characteristics.

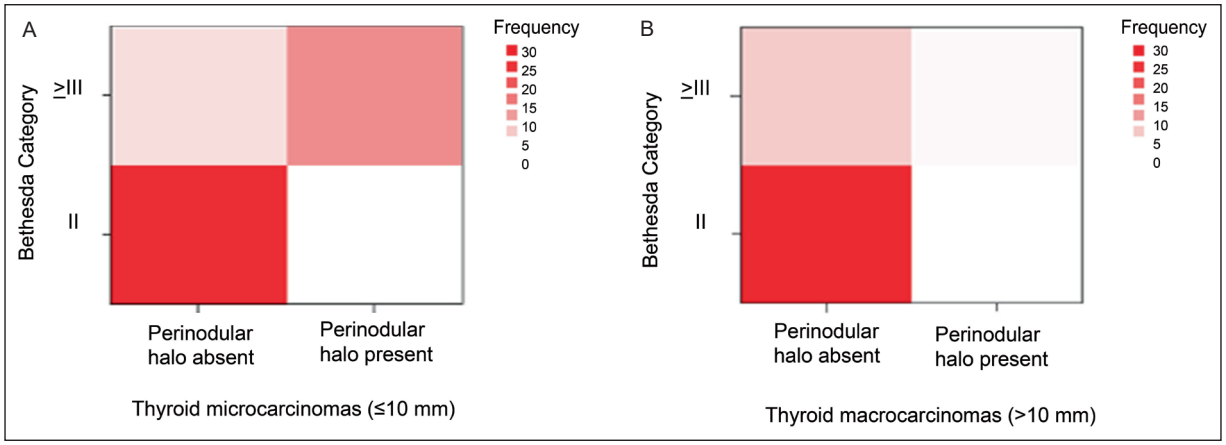

Figure 2. Heatmaps comparing the presence of a perinodular halo between thyroid microcarcinomas and macrocarcinomas using 2D-SWE. **A:** a perinodular halo was observed in microcarcinomas with Bethesda category ≥ III ($p < 0.001$). **B**: no association with perinodular halo was observed in thyroid macrocarcinomas.

2D-SWE: two-dimensional shear wave elastography.

and images were stored in the Picture Archiving and Communication System (PACS) (Carestream™, Health Inc., Rochester, NY, USA). The 2D-SWE color matrix was analyzed in two areas as defined by the authors (EC and MC). One area was obtained by placing the ROI in the intranodular parenchyma to determine the pure intrinsic stiffness of the nodule and the other was an extended area where the expanded ROI included intranodular tissue, capsule, and perinodular tissue of up to 2 mm outside the nodule boundary.

The size and location of the ROI were standardized. Before stabilizing and recording the image, we tried to obtain the best image to recognize all the characteristics of conventional grayscale US. The immediate elastographic acquisition with the map and color matrix included the entire nodule and the greatest amount of thyroid tissue surrounding it and away from its edges. In 2D-SWE acquisitions, the ROI was manipulated to include the nodule and at least 2 mm of surrounding tissue. A second ROI was located exclusively within the nodule. The reliability of elastography measurements was assessed using quality and propagation maps. Two radiologists (EC and MLC) with 35 and 6 years of experience performed the evaluations in double reading.

Thyroid biopsy

The thyroid nodule pathological diagnoses were categorized by FNAB according to the Bethesda System for Reporting Thyroid Cytopathology[7]. The material obtained was interpreted by a cytopathologist (LG) with 35 years of experience. The pathological diagnosis was confirmed by surgery.

Statistical analysis

The mean, standard deviation, minimum, maximum, and median were calculated for quantitative variables. The chi-square test or Fisher's exact test was used for categorical variables. Thyroid nodule size and its association with malignancy were analyzed using the Student's t-test and the Mann-Whitney U-test. The association between thyroid nodule stiffness by 2D-SWE and cytopathological Bethesda category was evaluated with the Shapiro-Wilk normality test. Receiving operating characteristics (ROC) curves with the area under the curve (AUC) defined the cutoff value for predicting malignancy of micronodules and macronodules. A p-value of < 0.05 was considered significant. The SPSS software version 25 (IBM Corp., Armonk, NY, USA) was used.

RESULTS

A total of 172 patients with thyroid nodules were evaluated, of whom 14 cases were excluded because FNAB samples were insufficient (n = 9) or surgical pathology results were unavailable (n = 5). Thus, 158 patients with 158 thyroid nodules were included. There were 131 women (82.9%) and 27 men (17.1%) with a mean age of 47.04 ± 14 years (range 13-85). A comparison of 64 micronodules and 94 macronodules with the TI-RADS, E-strain, and Bethesda system is shown in Table 1. Malignancy was confirmed in 58 (36.7%) of 158 nodules, of which 29 were thyroid microcarcinomas. The mean diameter of the microcarcinomas in US was 4.5 mm ± 0.9 mm. An E-strain pattern of 4 or 5 was found in 26 (89.6%) of the 29 microcarcinomas.

Thyroid nodule stiffness by 2D-SWE and cytopathological Bethesda category

The relationship between nodule stiffness by 2D-SWE and cytopathological findings is shown in Table 2. Bethesda II thyroid nodules had a median value of 18.0 kPa, Bethesda IV had 24.0 kPa, Bethesda V had 27.5 kPa, and Bethesda VI had 33.0 kPa ($p < 0.001$).

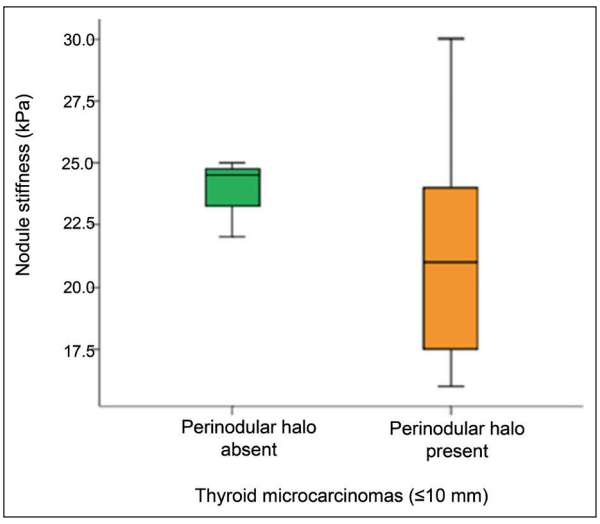

Figure 3. Boxplot showing the relationship between perinodular halo and nodular stiffness of thyroid microcarcinomas quantified by 2D-SWE. A perinodular halo was related to lower nodule stiffness values (softer micronodules).

2D-SWE: two-dimensional shear wave elastography.

Elastographic analysis showed higher stiffness values directly related to Bethesda categories III, IV, and V. Benign thyroid nodules had a median value of 12 ± 9.8 kPa. Malignant micronodules showed a median value of 25 ± 6.2 kPa compared to 32.9 ± 13.8 kPa for macronodules. 2D-SWE showed a wide range of values (5-64 kPa) for malignant macronodules. In contrast, a narrow range (18-35 kPa) was observed in benign nodules.

Diagnostic performance of the nodule stiffness cutoff value with 2D-SWE

ROC analyses for predicting malignancy based on thyroid nodule stiffness are shown in a three-group comparison: all thyroid nodules, micronodules, and macronodules (Figure 1). The cutoff value for nodule stiffness was 23.5 kPa to predict malignancy. Thyroid macronodules showed an AUC of 0.832 (95% CI 0.719-0.945), a sensitivity of 81.5%, and a specificity of 79.4%. In contrast, a cutoff value of 23.5 kPa for thyroid micronodules had an AUC of 0.664 (95% CI 0.517-0.810) with a sensitivity of 60.0% and a specificity of 35.7%.

Perinodular halo by 2D-SWE

The heatmaps in Figure 2 show the strong association between a rigid perinodular halo in thyroid microcarcinomas and Bethesda category III, IV, or V ($p < 0.001$)

Table 4. Comparison of the elastographic A/B index[a] by 2D-SWE in thyroid microcarcinomas with and without a perinodular halo

Thyroid microcarcinomas with perinodular halo, A/B index (n = 21)	Case 1	Case 2	Case 3	Case 4	Case 5	Case 6	Case 7	Case 8	Case 9	Case 10	Case 11
	1.35	1.33	1.40	1.33	1.34	1.55	1.70	1.73	1.80	1.40	1.95
	Case 12	Case 13	Case 14	Case 15	Case 16	Case 17	Case 18	Case 19	Case 20	Case 21	
	2.20	1.50	1.44	1.30	1.73	1.58	1.45	1.87	1.64	1.33	
Thyroid microcarcinomas without a perinodular halo, A/B index[b] (n = 8)	Case 1	Case 2	Case 3	Case 4	Case 5	Case 6	Case 7	Case 8			
	0.04	0.9	1.1	0.05	0.8	1.08	0.88	0.75			

[a]A/B index: (A) corresponds to the stiffness of an expanded ROI that includes the nodule + perinodular halo (up to 2 mm outside the limit of the nodule). (B) corresponds to the region of interest (ROI) of nodule stiffness; [b]The A/B index was only defined with the ROI of nodule stiffness. 2D-SWE: two-dimensional shear wave elastography.

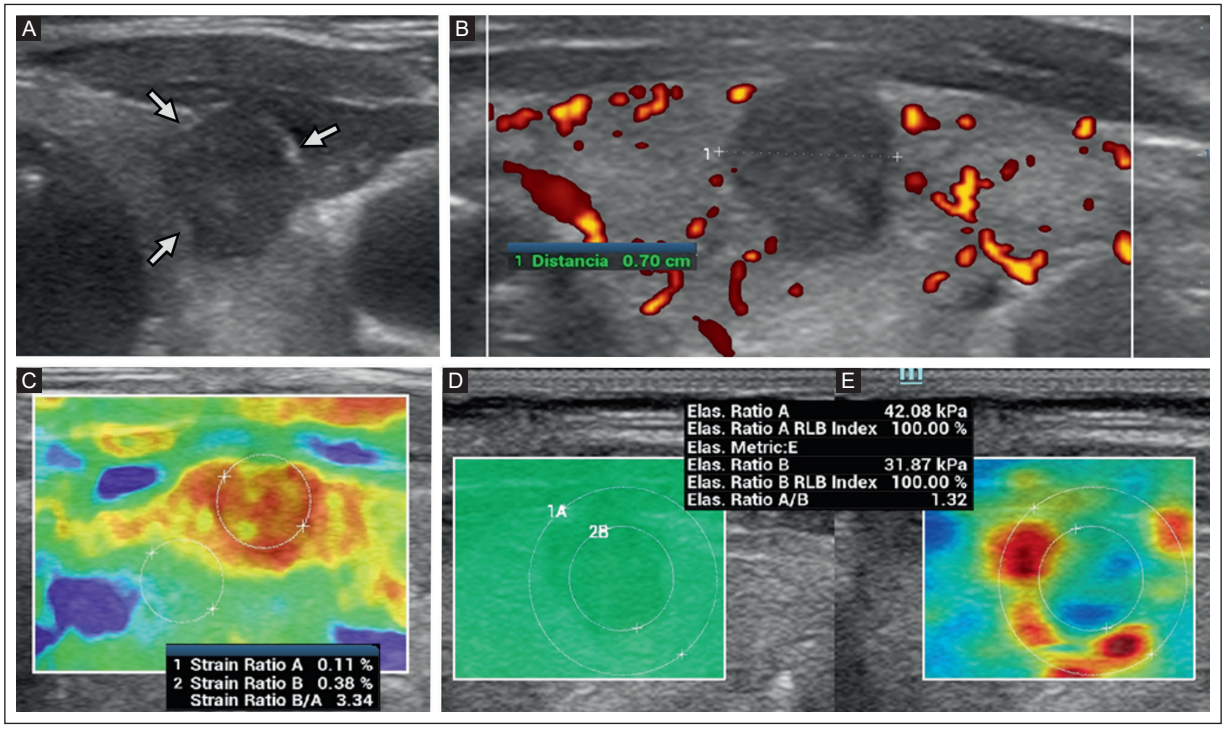

Figure 4. A 30-year-old woman with clinical symptoms of hypothyroidism and neck pain. **A:** grayscale US shows a 7-mm solid, hypoechoic micronodule, taller than wide, with a lobulated margin and peripheral microcalcifications (arrows). TI-RADS 5. **B:** color Doppler US with an absent intrinsic vascular signal and isolated, short, irregular peripheral vascular poles. **C:** E-strain without deformation (red map) and an area extending beyond the edge of the nodule (pattern 5). **D:** 2D-SWE quality map with a homogeneous green box confirming good acquisition. **E:** 2D-SWE color matrix showing a nodule with relative central nodular laxity (31 kPa) and a rigid perinodular halo (red ring) (42 kPa). The A/B index was 1.32. The FNAB was the Bethesda V category. The histopathological diagnosis was papillary thyroid microcarcinoma.

E-strain: elastography strain; FNAB: fine needle aspiration biopsy; kPa: kilopascals; TI-RADS: Thyroid Imaging Reporting and Data System; US: ultrasound; 2D-SWE: two-dimensional shear wave elastography.

in contrast to the absence of a perinodular halo in macrocarcinomas. Table 3 shows the association of nodule stiffness and perinodular halo in thyroid microcarcinomas using 2D-SWE. Notably, 21 (72.4%) of the 29 microcarcinomas with a perinodular halo had a median nodule stiffness of 21.0 kPa. In contrast, the median of 8 microcarcinomas without a perinodular halo was 24.5 kPa ($p < 0.001$) (Figure 3).

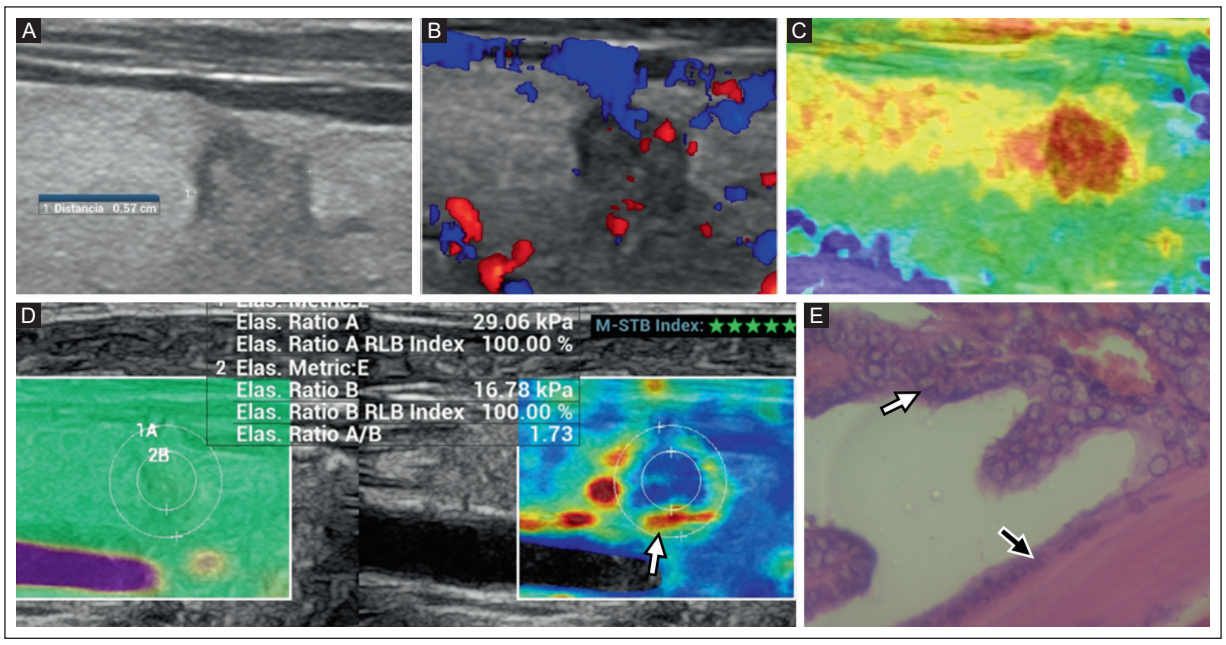

Figure 5. A 27-year-old woman with diabetes and a thyroid micronodule. **A:** grayscale US shows a 5-mm solid, hypoechoic, rounded micronodule with an angular margin. TI-RADS 4. **B:** a color Doppler US shows irregular vascular poles. **C:** E-strain shows pattern 4 (red) without compression deformation. **D:** 2D-SWE color matrix where nodular laxity is observed with a rigid perinodular halo (arrow). The relationship between A (29.1 kPa), configured by halo and nodule, and B (16.8 kPa), corresponding to the intrinsic stiffness of the nodule, results in an A/B index of 1.73. The FNAB was the Bethesda V category. **E:** surgical specimen (40× H&E) shows a thick capsule of scleral hyaline fibrous connective tissue (black arrow), accompanied by papillary protrusions (white arrow), lined by follicular cells, with overlapping and stacked nuclei, nuclear clefts, pseudo-inclusions, and nuclear folds (grooves). The histopathological diagnosis was papillary thyroid microcarcinoma.

E-strain: elastography-strain; FNAB: fine needle aspiration biopsy; H&E: hematoxylin-eosin; kPa: kilopascals; TI-RADS: Thyroid Imaging Reporting and Data System; US: ultrasound; 2D-SWE: two-dimensional shear wave elastography.

Elastographic stiffness by A/B index

A comparison of the elastographic stiffness index using 2D-SWE in thyroid microcarcinomas with and without a perinodular halo is shown in Table 4. The A/B index of microcarcinomas with a perinodular halo was 1.56 ± 0.23, compared to those without a halo (0.7 ± 0.39). A stiffness A/B index ≥ 1.3 was found in all microcarcinomas with a perinodular halo (n = 21, 100%). Figures 4–7 are examples of 2D-SWE features, E-strain, and conventional US with TI-RADS 4 or 5, respectively.

Elastographic patterns of thyroid microcarcinomas

Although the study's sample size was small, we consider it feasible to propose the integration of 2D-SWE features, E-strain, and conventional US with TI-RADS 4 or 5 to define three elastographic patterns of thyroid microcarcinomas (Table 5; Figure 8).

Congruent elastographic pattern: concordance of conventional US with TI-RADS 4 or 5, E-strain with pattern 4 or 5, and 2D-SWE with nodule stiffness ≥ 23.5 kPa without a perinodular halo and an A/B index < 1.3.

Incongruent elastographic pattern: conventional US with TI-RADS 4 or 5, E-strain with pattern 4 or 5, and discordant findings on 2D-SWE with intrinsic thyroid nodule laxity (< 23.5 kPa), the presence of a rigid perinodular halo, and an A/B index ≥ 1.3.

Atypical congruent elastographic pattern: conventional US with TI-RADS 4 or 5, atypical findings on E-strain with patterns 1, 2, or 3, and 2D-SWE with intrinsic nodular laxity (< 23.5 kPa), the presence of a rigid perinodular halo, and an A/B index ≥ 1.3.

These three patterns highlight the importance of assessing the nodular and perinodular stiffness of the tissue using the 2D-SWE color matrix, which may have a different expression depending on the size of the nodule, its intrinsic structural composition, and desmoplastic changes.

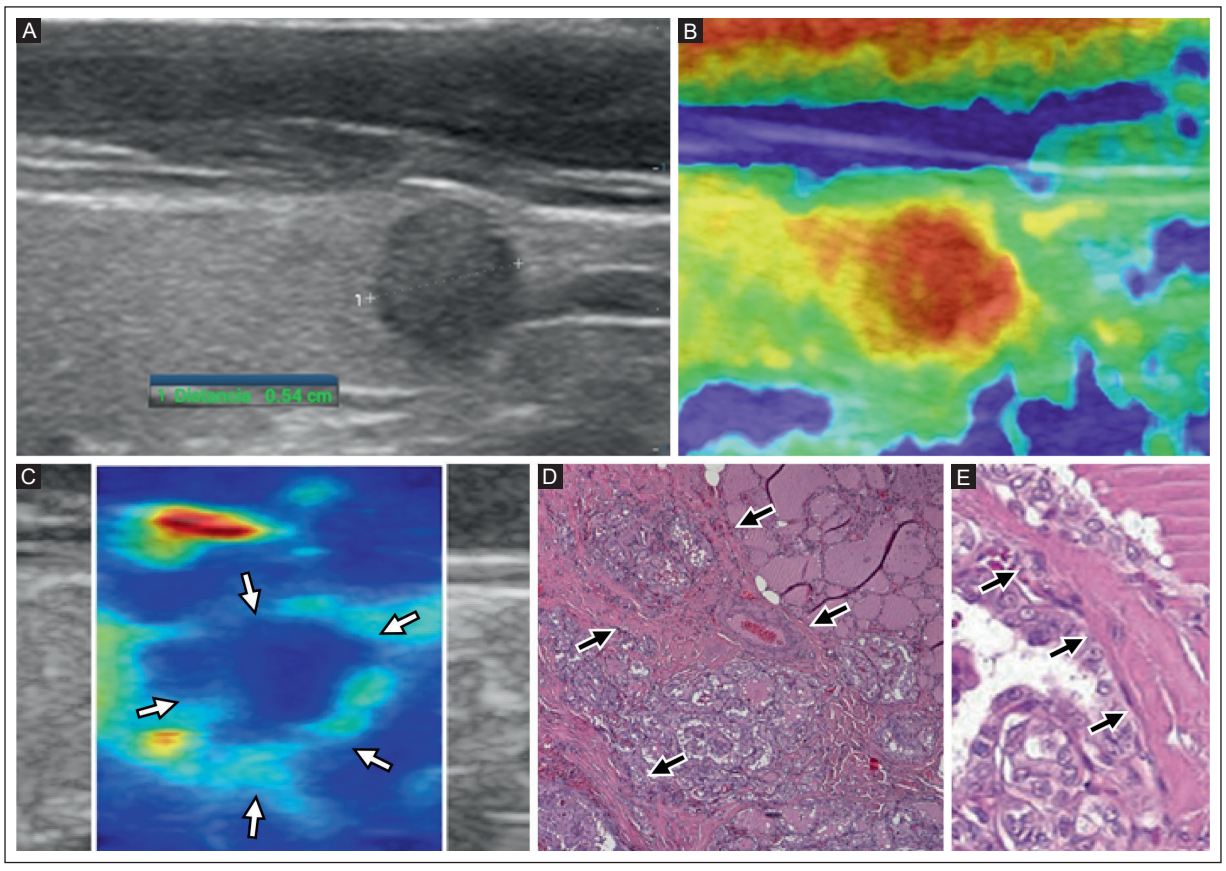

Figure 6. A 35-year-old asymptomatic man with an incidental thyroid nodule. **A:** grayscale US shows a 5-mm solid, hypoechoic, round, homogeneous micronodule with a lobulated margin. TI-RADS 4. **B:** E-strain shows the nodule without deformation (red), pattern 4. **C:** the 2D-SWE color matrix shows a nodule stiffness of 12 kPa (blue color) bordered by a perinodular stiffness halo of 18 kPa (arrows). The A/B index was 1.5. The FNAB was the Bethesda V category. **D:** surgical specimen (40× H&E) with a significant reaction of the desmoplastic stroma (arrows) surrounding the nests of intratumoral cells. **E:** peritumoral desmoplastic reaction (arrows). The histopathological diagnosis was papillary thyroid microcarcinoma.

E-strain: elastography-strain; FNAB: fine needle aspiration biopsy; kPa: kilopascals; H&E: hematoxylin-eosin; TI-RADS: Thyroid Imaging Reporting and Data System; US: ultrasound; 2D-SWE: two-dimensional shear wave elastography.

DISCUSSION

This study showed that the combination of 2D-SWE features such as nodule stiffness, perinodular halo, A/B index, and matrix color has a differential expression in thyroid microcarcinomas. Three elastographic patterns, namely, congruent, incongruent, and atypical congruent, are based on the thyroid microcarcinoma findings by conventional US, E-strain, and 2D-SWE. These elastographic patterns have not been described in the literature.

Thyroid nodule stiffness has been related to cell density, colloid content, and intrinsic and perinodular fibrosis. Therefore, the tissue stiffness variability measured by 2D-SWE may reflect the heterogeneous architecture and density of fibrillar collagen in thyroid nodules. Duan et al.[9] recommended the quantitative 2D-SWE assessment for diagnosing thyroid microcarcinoma, but their study did not include 2D-SWE color matrix assessment or conventional US findings. On the other hand, Zhang et al.[10] and Hu et al.[11] evaluated the 2D-SWE color matrix to quantify nodule stiffness and emphasized the relevance of elastographic characteristics of the tissue at the edge of the nodule. We propose three elastographic patterns that optimize the use of elastographic features of thyroid microcarcinomas with different biological behaviors. The congruent elastographic pattern is characterized by the concordance of conventional US with TI-RADS 4 or 5, E-strain without deformation (pattern 4 or 5), and 2D-SWE with a nodule stiffness ≥ 23.5 kPa without a perinodular halo, and an A/B index < 1.3. Intrinsic nodule stiffness can predict malignant thyroid microcarcinoma.

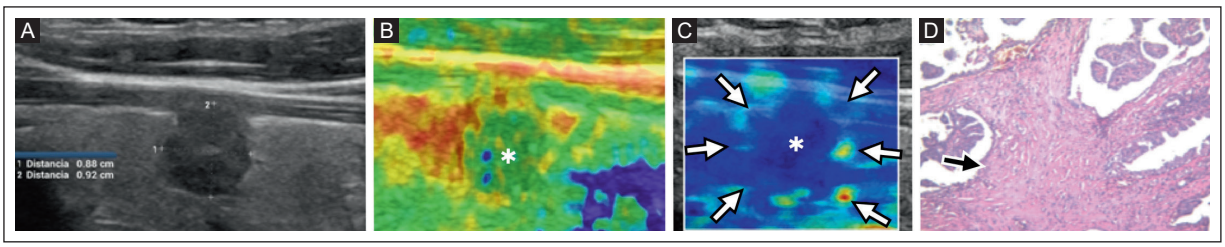

Figure 7. A 28-year-old woman with a family history of thyroid cancer. **A:** grayscale US examination shows a 8-mm solid, hypoechoic, taller than wide, micronodule with an irregular and lobulated margin. TI-RADS 5. **B:** E-strain shows a discrete reverberation (red) surrounding the micronodule (asterisk), which has a color map pattern 1 (green) with a non-deformable perimeter ring (yellow). **C**: 2D-SWE color matrix with nodule stiffness of 9 kPa (asterisk) and a rigid perinodular halo (arrows), with 13 kPa and an A/B index of 1.44. The FNAB was the Bethesda V category. **D:** surgical specimen (400× H&E) shows the tumor matrix with papillary protrusions lined by follicular cells with abundant acellular fibrosclerosis (arrow). The histopathological diagnosis was papillary thyroid microcarcinoma.

E-strain: elastography strain; FNAB: fine needle aspiration biopsy; H&E: hematoxylin-eosin; kPa: kilopascals; TI-RADS: Thyroid Imaging Reporting and Data System; US: ultrasound; 2D-SWE: two-dimensional shear wave elastography.

Table 5. Thyroid microcarcinoma elastographic patterns according to conventional US with TI-RADS 4 or 5, E-strain, and 2D-SWE

Description	TI-RADS category	E-strain pattern	2D-SWE		
			Thyroid nodule stiffness (kPa)	Perinodular halo	A/B index[a]
Congruent elastographic pattern	4 or 5	4 or 5	≥ 23.5	Absent	< 1.3
Incongruent elastographic pattern	4 or 5	4 or 5	< 23.5	Present	≥ 1.3
Atypical congruent elastographic pattern	4 or 5	1, 2 or 3	< 23.5	Present	≥ 1.3

[a]A/B index: (A) corresponds to the stiffness of an expanded region of interest (ROI) that includes the nodule + perinodular halo (up to 2 mm outside the limit of the nodule), and (B) corresponds to the ROI of nodule stiffness; TI-RADS: Thyroid Imaging Reporting and Data System; kPa: kilopascals; E-Strain: elastography strain; 2D-SWE: two-dimensional shear wave elastography; US: ultrasound.

In contrast, the incongruent elastographic pattern was found in fibrosclerotic lesions with a perimetral desmoplastic reaction associated with apparent intrinsic softness of the nodule and a rigid perinodular halo, with an A/B index ≥ 1.3, and E-strain without deformation (pattern 4 or 5). The apparent laxity of thyroid microcarcinomas may suggest benignity if only tissue stiffness is assessed. In contrast, microcarcinomas with an atypical congruent elastographic pattern were visualized with E-strain "mirrored with 2D-SWE color matrix," i.e., apparent intrinsic nodular laxity with a rigid perinodular halo in both elastographic modalities and conventional US with TI-RADS 4 or 5. The histopathological features of this elastographic pattern showed infiltrative behavior of adjacent tissue and angiolymphatic invasion with peripheral desmoplasia that restricts the elastogram. 2D-SWE features such as thyroid nodule stiffness quantification, the presence of a perinodular halo, and color matrix features to determine the halo/nodule A/B index can be evaluated in patients with thyroid micronodules and may be useful for diagnosing thyroid microcarcinoma.

There is no defined cutoff value for tissue stiffness measured by 2D-SWE to differentiate between benign and malignant thyroid nodules[11]. It has been suggested that stiffness is lower in thyroid micronodules than macronodules[1]. Published studies report a wide range of stiffness values between 19 and 85 kPa.[1,2,11-16]. This wide range may be related to differences in the equipment, volume, and histological type of the thyroid nodule. In our study, the accuracy of the ≥ 23.5 kPa cutoff value of nodule stiffness was higher in macrocarcinomas (AUC 0.832) than in microcarcinomas (AUC 0.664). 2D-SWE appears to have lower diagnostic accuracy in microcarcinomas, especially those with apparent intrinsic softness (< 23.5 kPa) that have a rigid perinodular halo. Based on our results, we believe that in the assessment of thyroid micronodules, nodule stiffness quantification using 2D-SWE should be combined with other elastographic features such as perinodular halo, A/B index, and color matrix to increase the accuracy of thyroid microcarcinoma diagnosis.

Few published studies analyze the diagnostic relevance of the rigidity of the perinodular halo for the

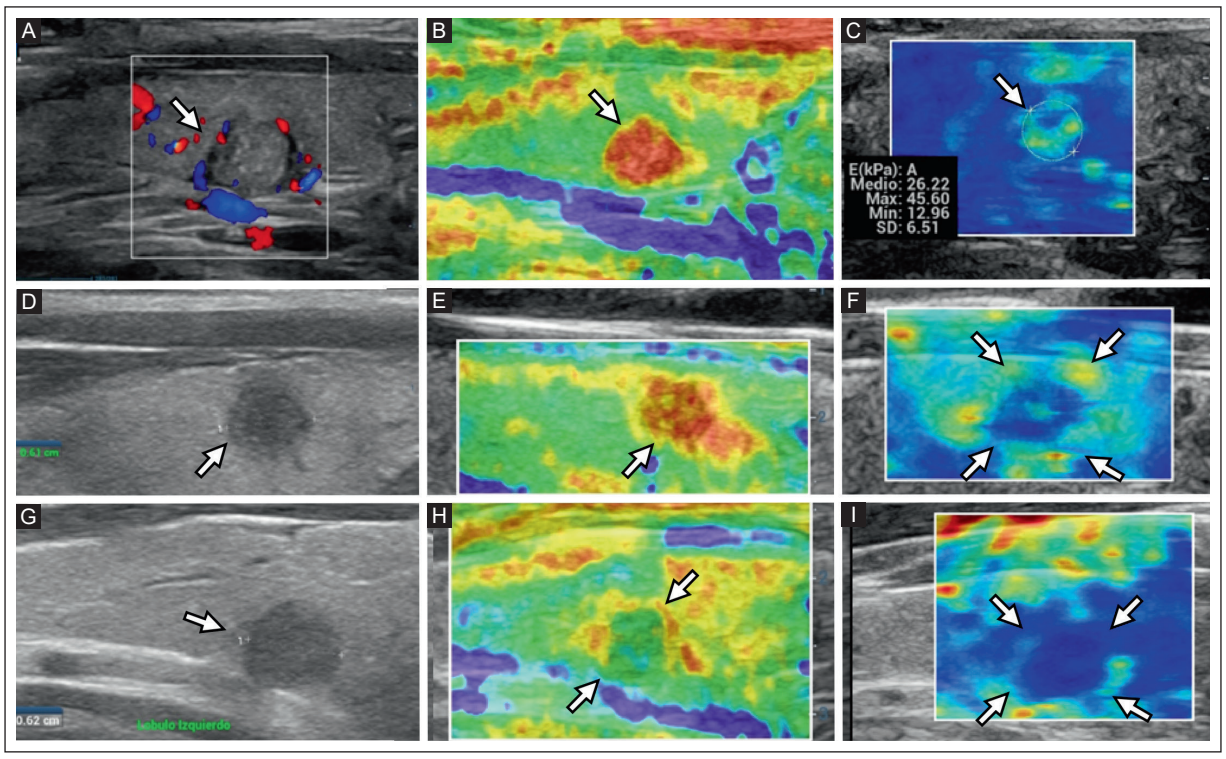

Figure 8. Three proposed elastographic patterns based on combined grayscale US, E-strain, and 2D-SWE features. *Congruent elastographic pattern (upper panel).* **A:** grayscale US showing a 6-mm solid, hypoechoic (arrow), rounded micronodule with an irregular margin and calcifications with peripheral vessels. TI-RADS 5. **B:** E-strain without deformation (pattern 4). The color map shows an intense red nodule (arrow). **C:** 2D-SWE color matrix shows ROI (arrow) with a nodular stiffness of 26.2 kPa. A perinodular halo is not present. The FNAB was the Bethesda V category. The histopathological diagnosis was papillary thyroid microcarcinoma. *Incongruent elastographic pattern (middle panel)* **D:** grayscale US shows a 6-mm solid, hypoechoic, rounded micronodule with an irregular margin (arrow). TI-RADS 5. **E**: E-strain without deformation (pattern 4) shows a red nodule (arrow). **F:** 2D-SWE color matrix shows a blue nodule with a stiffness of 15 kPa and a rigid ring represented by a light blue halo with orange-red spots (27 kPa) (arrows). The A/B index was 1.8. The FNAB was the Bethesda III category. The histopathological diagnosis was papillary thyroid microcarcinoma. *Atypical congruent elastographic pattern (lower panel)* **G:** grayscale US shows a 6-mm solid, hypoechoic, rounded micronodule with an irregular margin (arrow) with extrathyroidal extension with border abutment, contour bulging, or loss of the echogenic thyroid border, TI-RADS 5. **H:** E-strain pattern 1 of the micronodule (green core) with a thin, non-deformable (red) perinodular halo (arrows). The strong stiffness of the halo restricts the intrinsic expression of nodule stiffness. **I:** 2D-SWE with a nodule stiffness of 12.0 kPa, color matrix with a blue nodule (apparent intrinsic laxity), and a light blue perinodular halo (arrows). The A/B index was 1.33. The FNAB was the Bethesda V category. The histopathological diagnosis was papillary thyroid microcarcinoma.

E-strain: elastography strain; FNAB: fine needle aspiration biopsy; kPa: kilopascals; ROI: region of interest; TI-RADS: Thyroid Imaging Reporting and Data System; US: ultrasound; 2D-SWE: two-dimensional shear wave elastography.

differential diagnosis of benign and malignant thyroid nodules[1,6]. In our study, perinodular halo stiffness was significantly higher in malignant nodules than in benign nodules. We hypothesize that a rigid perinodular halo modifies elastographic behavior and can dissemble or reduce the intrinsic rigidity of microcarcinomas. In several malignant thyroid micronodules, maximum stiffness was observed in the perinodular region and not in the lesion. Microcarcinomas, in which there was a halo, appeared intrinsically softer. The inaccuracy of 2D-SWE in microcarcinomas with apparent intrinsic softness is compensated by analyzing the 2D-SWE color matrix to quantify intra- and perinodular stiffness, with the determination of the halo/nodule elastographic index (A/B index). In this context, it is possible that the degree of perinodular fibrosis disturbs the real intrinsic plasticity of the nodule and consequently modifies the expression of the 2D-SWE color matrix, and the quantitative value of stiffness.

The strengths of this study include the fact that all benign and malignant thyroid nodules were targeted using FNAB, which is the reference standard, and were evaluated with conventional US and two complementary elastographic modalities by experienced neck radiologists. Study limitations include the retrospective, single-center design, and a small sample

size. The follow-up to determine the clinical behavior associated with the proposed elastographic patterns has not been included. On the other hand, no comparisons of elastographic patterns with macronodules have been made. Although the quantification data are objective, interobserver and intraobserver agreement was not determined, which is important considering that elastography has operator-dependent variability. Although 2D-SWE depends less on the operator, some factors can affect the spread through the tissue, so it is recommended to apply objective parameters and quality indicators and seek good training and experience in order to issue ultrasound elastography reports.

CONCLUSION

The three elastographic patterns are based on the combination of conventional US, E-strain patterns, and data provided by 2D-SWE by quantifying nodule stiffness, the presence of a perinodular halo, and characteristics of the color matrix to determine the A/B index (halo/nodule). The three elastographic patterns can be useful for diagnosing thyroid microcarcinoma, especially in cases with TI-RADS 4 or 5 and indeterminate cytopathology. US elastography is painless and requires only a few additional minutes without special preparation for patients. Further research is needed to confirm the results of this study and evaluate the diagnostic performance of elastographic patterns in large multicenter prospective cohort studies.

Acknowledgments

The authors thank Professor Ana M. Contreras-Navarro for her guidance in preparing and writing this scientific paper. We also appreciate the support of the Endocrinology Service of the National Hospital of Clinics – Faculty of Medical Sciences of the National University of Cordoba and the Society of Endocrinology and Metabolism of the Province of Cordoba, Argentina.

Funding

This research received no external funding.

Conflicts of interest

The authors declare no conflicts of interest.

Ethical disclosures

Protection of individuals. This study complies with the Declaration of Helsinki (1964) and its amendments.

Confidentiality of data. The authors declared that they followed their center's protocol for sharing patient data.

Right to privacy and informed consent. Informed consent was not required for this observational study of information collected during routine clinical care.

Use of artificial intelligence. The authors state that they did not use generative artificial intelligence to prepare this manuscript and/or create tables, figures, or figure legends.

REFERENCES

1. Tan S, Sun PF, Xue H, Fu S, Zhang ZP, Mei F, et al. Evaluation of thyroid micro-carcinoma using shear wave elastography: Initial experience with qualitative and quantitative analysis. Eur J Radiol. 2021;137:109571. doi:10.1016/j.ejrad.2021.109571.
2. Zhao CK, Xu HX. Ultrasound elastography of the thyroid: principles and current status. Ultrasonography. 2019;38(2):106-124. doi: 10.1016/j.ultras.2014.04.027.
3. Faquin WC, Baloch ZW. Fine-needle aspiration of follicular patterned lesions of the thyroid: Diagnosis, management, and follow-up according to National Cancer Institute (NCI) recommendations. Diagn Cytopathol. 2010; 38(10):731–739. doi: 10.1002/dc.21292.
4. Mehrotra P, McQueen A, Kolla S, Johnson SJ, Richardson DL. Does elastography reduce the need for thyroid FNAs? Clin Endocrinol (Oxf). 2013; 78(6):942–949. doi: 10.1111/cen.12077.
5. Wang Y, Dan HJ, Dan HY, Li T, Hu B. Differential diagnosis of small single solid thyroid nodules using real-time ultrasound elastography. J Int Med Res. 2010;38(2):466-72. doi: 10.1177/147323001003800210.
6. Hu L, He NA, Xie L, Ye X, Liu X, Pei C, et al. Evaluation of the Perinodular Stiffness Potentially Predicts the Malignancy of Thyroid Nodules. J Ultrasound Med. 2020; 39(11):2183-2193. doi: 10.1002/jum.15329.
7. Civas ES, Ali SZ. The Bethesda System for Reporting Thyroid Cytopathology. Am J Clin Pathol. 2009;132:658-665. doi: 10.1309/AJCPPHLWMI3JV4LA.
8. Rago T, Vitti P. Role of thyroid ultrasound in the diagnostic evaluation of thyroid nodules. Best Pract Res Clin Endocrinol Metab. 2008; 22(6):913-928. doi:10.1016/j.beem.2008.09.016.
9. Duan SB, Yu J, Li X, Han ZY, Zhai HY, Liang P. Diagnostic value of two-dimensional shear wave elastography in papillary thyroid microcarcinoma. Onco Targets Ther. 2016;9(9):1311-1317. doi: 10.2147/OTT.S98583.
10. Zhang YX, Xue JP, Li HZ, Miao JW, Kang CS. Clinical Value of Shear Wave Elastography Color Scores in Classifying Thyroid Nodules. Int J Gen Med. 2021;14:8007-8018. doi: 10.2147/IJGM.S331406.
11. Hu L, He N, Ye L, Zhou H, Zhong W, Zhang X. Evaluation of the Stiffness of Tissues Surrounding Thyroid Nodules with Shear Wave Elastography. J Ultrasound Med. 2018; 37(9):2251-2261. doi: 10.1002/jum.14578.
12. Liang XW, Cai YY, Yu JS, Liao JY, Chen ZY. Update on thyroid ultrasound: a narrative review from diagnostic criteria to artificial intelligence techniques. Chin Med J (Engl). 2019;132(16):1974-1982. doi: 10.1097/CM9.0000000000000346.
13. Kim H, Kim JA, Son EJ, Youk JH. Quantitative assessment of shear-wave ultrasound elastography in thyroid nodules: diagnostic performance for predicting malignancy. Eur Radiol. 2013;23(9):2532–2537. doi: 10.1007/s00330-013-2847-5.
14. Moon HJ, Kim EK, Yoon JH, Kwak JY. Clinical implication of elastography as a prognostic factor of papillary thyroid microcarcinoma. Ann Surg Oncol. 2012;19(7):2279–2287. doi: 10.1245/s10434-011-2212-3.
15. Fukuhara T, Matsuda E, Fujiwara K, Tanimura C, Izawa S, Kataoka H, et al. Phantom experiment and clinical utility of quantitative shear wave elastography for differentiating thyroid nodules. Endocr J. 2014;61(6):615-621. doi:10.1507/endocrj.ej14-0061.
16. Zhang YX, Xue JP, Li HZ, Miao JW, Kang CS. Clinical Value of Shear Wave Elastography Color Scores in Classifying Thyroid Nodules. Int J Gen Med. 2021;14:8007-8018. doi: 10.2147/IJGM.S331406.